Multicomponent Polymerizations of Alkynes, Sulfonyl Azides, and 2-Hydroxybenzonitrile/2-Aminobenzonitrile toward Multifunctional Iminocoumarin/Quinoline-Containing Poly(N-sulfonylimine)s

Liguo Xu,[†] Taotao Zhou,[†] Min Liao,[†] Rongrong Hu,*,[†] and Ben Zhong Tang*,[†,‡]

[†]State Key Laboratory of Luminescent Materials and Devices, Center for Aggregation-Induced Emission, South China University of Technology, Guangzhou 510640, China

[‡]Department of Chemistry, Hong Kong Branch of Chinese National Engineering Research Centre for Tissue Restoration and Reconstruction, The Hong Kong University of Science and Technology, Clear Water Bay, Kowloon, Hong Kong, China

S Supporting Information

ABSTRACT: Multicomponent polymerizations (MCPs) provide a powerful synthetic tool for the construction of polymers with complex structures and multifunctionalities, owing to their great structural diversity, mild condition, high efficiency, simple procedure, and environmental benefit. They possess significant advantages in synthesizing heteroatom-rich or heterocycle-containing functional polymers through directly constructing fused heterocycles from the MCP. In this work, the MCPs of diynes, disulfonyl azides, and 2-hydroxybenzonitrile or 2-aminobenzonitrile were reported under the catalysis of CuCl and Et$_3$N, generating iminocoumarin/quinoline-containing poly(N-sulfonylimine)s with high molecular weights (up to 37700 g/mol) and high yields (up to 96%). The MCPs enjoy a wide monomer scope and high atom economy, releasing N$_2$ as the only byproduct. The fluorescent poly(N-sulfonylimine) can be utilized for sensitive and selective detection of Ru^{3+}, which also possesses antibacterial properties. The efficient MCPs could produce polymers with unique structures and functionalities, thereby accelerating the development of polymer materials.
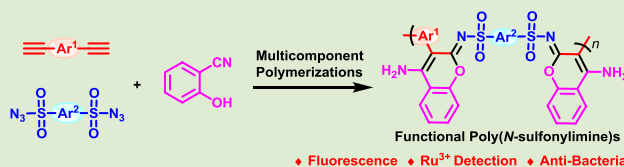
The development of polymerization methodologies is essential for the exploration of new polymer materials. Recently, multicomponent polymerizations (MCPs) emerged as popular synthetic methods, which have attracted much attention owing to their great structural diversity, mild reaction condition, high efficiency, simple procedure, and environmental benefit.[1−5] For example, a few MCPs have been developed, such as Passerini 3-component polymerization and Ugi 4-component polymerization,[6−8] bringing polyesters and polyamides with diverse chemical and topological structures. Recent progress on the multicomponent tandem polymerizations (MCTPs) has extended the general applicability of MCPs and enriched the product structure of MCPs to conjugated polymers as well as sequence-controlled polymers.[9−11] The elemental sulfur-based MCPs have also demonstrated their practical implications of direct conversion from the abundantly existing sulfur to functional polythioamides or polythioureas in economic, efficient, and convenient manners.[12,13]

Of all the reported MCPs, the alkyne and sulfonyl azide-involving MCPs are a group of fascinating polymerizations with various product structures.[14−18] These MCPs are normally conducted at room temperature with the catalysis of copper(I), producing products with high yields and high molecular weights (M_ws), releasing N$_2$ as the only byproduct, demonstrating wide monomer applicability and high atom utilization. Most importantly, these MCPs can produce heteroatom-rich or fused heterocyclic ring-containing polymers

with multifunctionalities that are difficult to be accessed by other synthetic methods.

Among fused heterocycles, iminocoumarin and quinoline derivatives are widely available in nature, which are well-known for their fluorescence properties[19] and versatile biological activities, such as antibacterial,[20] antituberculosis,[21] anti-HIV,[22] anticancer effects,[23] and protein-tyrosine kinase inhibitors.[24] The iminocoumarin or quinoline-containing polymers have hence attracted considerable attention, owing to their potential functionalities. Their preparation, however, remains quite challenging, which usually involves a multistep synthesis and harsh conditions. For example, quinoline-containing polyfluorenes and poly(arylene ethynylene)s are reported through Friedländer quinolone synthesis and transition metal-catalyzed polycouplings from quinoline-containing monomers, respectively.[25,26] One example of the direct construction of iminocoumarin moieties is from the MCP of diynes, disulfonyl azides, and salicylaldehyde/o-hydroxylacetophenone to produce poly(iminocoumarin)s.[27]

Most recently, efficient multicomponent reactions (MCRs) of alkynes, sulfonyl azides, and 2-hydroxybenzonitrile or 2-aminobenzonitrile were reported to produce a library of multisubstituted 4-amino-iminocoumarins or 4-aminoquino-

lines.[28,29] In the MCR, terminal alkyne first reacts with sulfonyl azide under the catalysis of CuCl and Et$_3$N to form keteneimine **A** (Scheme S1). 2-Hydroxybenzonitrile is deprotonated by triethylamine to form nucleophile **B**, which then attacks keteneimine **A** to produce intermediate **C**. Subsequently, an intramolecular cyclization of **C** takes place to form the anionic species **D**, followed by protonation and isomerization to produce amino-substituted iminocoumarin **F**. A similar mechanism applies for the MCR of alkyne, sulfonyl azide, and 2-aminobenzonitrile, which produces amino-substituted quinoline.

Attracted by the straightforward construction of iminocoumarin or quinoline structures, in this work, we developed two efficient MCPs of diynes, disulfonyl azides, and 2-hydroxybenzonitrile or 2-aminobenzonitrile to generate poly(*N*-sulfonylimine)s with well-defined structures, high M_ws and yields under mild condition. The unique structures of the iminocoumarin/quinoline-containing poly(*N*-sulfonylimine)s endow them with good thermal stability, unique fluorescence, sensitive and selective detection of Ru^{3+}, and antibacterial property.

To develop the MCP of alkyne, sulfonyl azide, and 2-hydroxybenzonitrile, aromatic diyne monomer **1a** and disulfonyl azide monomer **2a** were designed and synthesized to polymerize with commercially available 2-hydroxybenzonitrile **3** upon the catalysis of CuCl and Et$_3$N under a N$_2$ atomosphere.[30−32] The solvent effect of the MCP of **1a**, **2a**, and **3** was first studied (Table S1). Of all the tested solvents, CH$_2$Cl$_2$ provides the best polymerization result, with 83% yield and a M_w of 23100 g/mol of the product. Monomer concentration possesses great influence on the polymerization (Table S2). When the concentrations of **1a** and **2a** were beyond 0.10 M while keeping [**1a**]/[**2a**]/[**3**] = 1.0/1.0/2.5, insoluble gel was easily formed within 30 min. Decreasing the concentrations to 0.05 M avoided the gelation and produced soluble product with satisfactory yield and M_w in 1 h. Further decreasing the concentration led to dramatic drop of both yield and M_w. Prolonging the reaction time generally increased the yields and M_ws (Table S3). A soluble polymer with a M_w of 34700 g/mol could be gained in 1.5 h in 95% yield, and an insoluble gel could form afterward. Although an excess amount of **3** proved to benefit the polymerization, from the strict stoichiometric ratio of [**1a**]/[**2a**]/[**3**] = 1.0/1.0/2.0, a satisfactory result with 91% yield and a M_w of 29300 g/mol was also obtained (Table S4). This MCP proceeded smoothly at room temperature, which was further improved upon raising the temperature until gelation occurred at 50 °C. The best polymerization result was realized at 40 °C in CH$_2$Cl$_2$ with the optimal monomer concentrations of [**1a**] = [**2a**] = 0.05 M and the molar ratio of [**1a**]/[**2a**]/[**3**] = 1.0/1.0/2.5, and polymer with a M_w of 35500 g/mol was produced in 96% yield in 1.5 h (Table S5). Insoluble gel could be formed in CH$_2$Cl$_2$ with higher monomer concentration, longer polymerization time, or higher polymerization temperature than the optimal condition, due to the existence of abundant and multiple types of intermolecular noncovalent interactions including hydrogen bonds and π−π stacking interactions in polymer product with high M_ws.

Various aromatic diyne monomers **1a−e** and disulfonyl azide monomers **2a,b** were synthesized for the MCP. Under
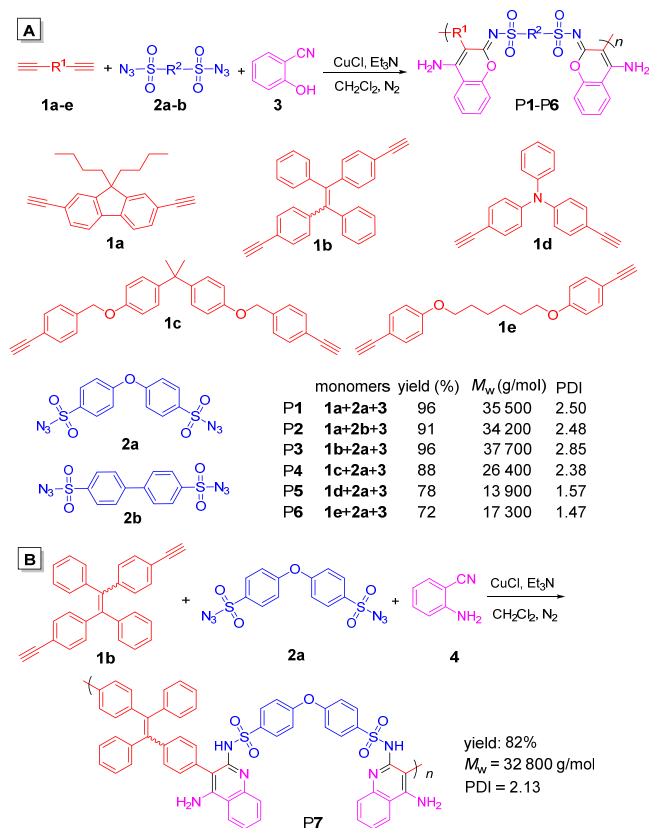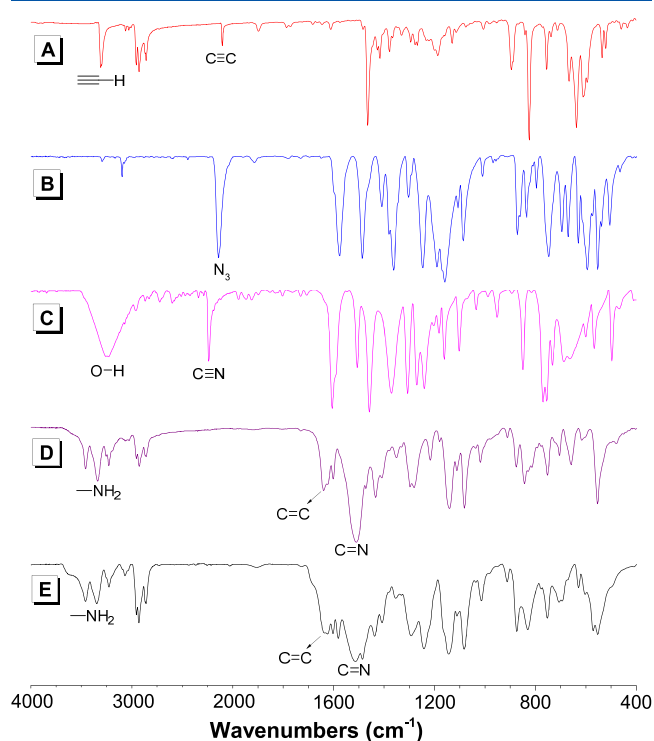

Figure 1. Cu(I)-catalyzed MCPs of diynes, disulfonyl azides, and (A) 2-hydroxybenzonitrile or (B) 2-aminobenzonitrile. The MCPs were carried out at 40 °C for 1.5 h (**P1**−**P6**) or 0.5 h (**P7**). M_ws are measured by GPC in DMF based on PMMA standard samples.

monomers	yield (%)	M_w (g/mol)	PDI
P1 **1a**+**2a**+**3**	96	35 500	2.50
P2 **1a**+**2b**+**3**	91	34 200	2.48
P3 **1b**+**2a**+**3**	96	37 700	2.85
P4 **1c**+**2a**+**3**	88	26 400	2.38
P5 **1d**+**2a**+**3**	78	13 900	1.57
P6 **1e**+**2a**+**3**	72	17 300	1.47

yield: 82%
M_w = 32 800 g/mol
PDI = 2.13

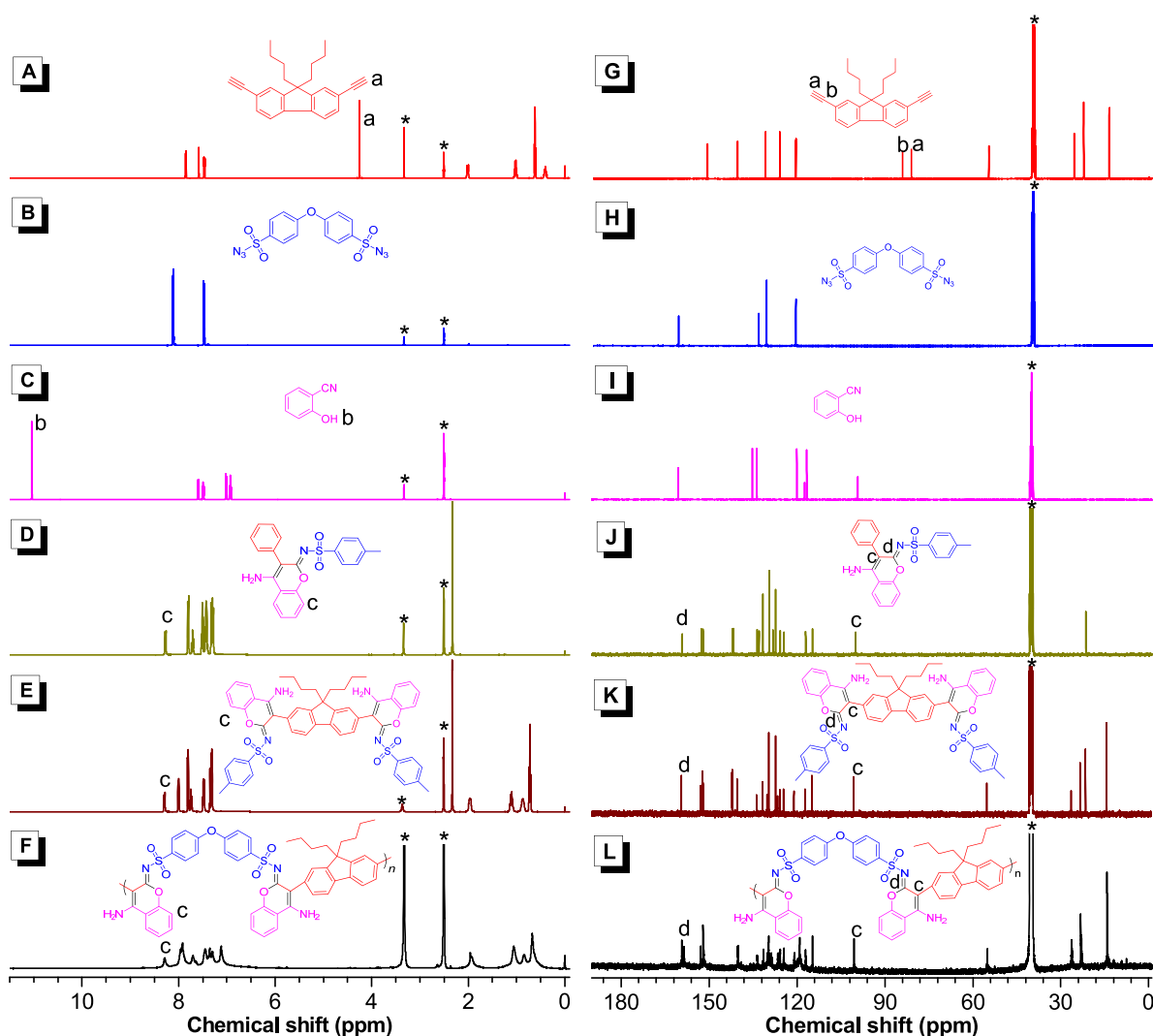**Figure 2.** IR spectra of (A) **1a**, (B) **2a**, (C) **3**, (D) **8**, and (E) **P1**.

Figure 3. ^{1}H NMR spectra of (A) **1a**, (B) **2a**, (C) **3**, (D) **7**, (E) **8**, and (F) **P1** in DMSO-d_6. ^{13}C NMR spectra of (G) **1a**, (H) **2a**, (I) **3**, (J) **7**, (K) **8**, and (L) **P1** in DMSO-d_6. The peaks marked with asterisks are from solvent.

the above-mentioned optimal condition, the polymerizations went smoothly and afforded **P1**−**P6** with M_ws up to 37700 g/mol in good to excellent yields (Figure 1A). Furthermore, when 2-hydroxybenzonitrile **3** was replaced by 2-aminobenzonitrile **4** in the MCP, the polymerization of **1b**, **2a**, and **4** also proceeded efficiently, furnishing aminoquinoline-containing poly(*N*-sulfonylimine) **P7** with a M_w of 32800 g/mol in 82% yield in 0.5 h (Figures 1B and S1), demonstrating the general monomer applicability of this MCP.

The model compounds **7**−**9** were obtained to help the characterization of chemical structures of **P1**−**P7** (Scheme S2), and their desired structures were confirmed by high resolution mass spectra (Figures S2−S4). The IR, ^{1}H NMR, and ^{13}C NMR spectra were utilized to compare the structures of monomers, model compounds, and polymers. In the IR spectra of **8** and **P1**, the absorption bands related to the ≡C—H and C≡C stretching vibrations of **1a** at 3307 and 2104 cm^{−1}, respectively, the N₃ stretching vibration band of **2a** at 2142 cm^{−1}, and the absorption bands associated with the −OH and C≡N stretching vibrations of **3** at 3246 and 2236 cm^{−1}, respectively, all disappeared, suggesting the total consumption of monomers. New −NH₂ peaks at 3458 and 3337 cm^{−1}, C═C peak at 1640 cm^{−1}, and C═N peak at 1511 cm^{−1} emerged

in the spectra of **8** and **P1**, confirming the expected amino-substituted iminocoumarin structure in these compounds (Figure 2). Similarly, these characteristic product peaks also emerged in the IR spectra of **P2**−**P7**, proving the expected structures of these polymers (Figures S5 and S6).

The ^{1}H and ^{13}C NMR spectra of monomers, model compounds, and **P1** were compared in Figure 3. In the ^{1}H NMR spectra of **7**, **8**, and **P1**, the acetylene proton resonance of **1a** at δ 4.25 and the phenolic hydroxyl proton resonance of **3** at δ 11.04 are both absent. Besides, a new peak emerged at δ 8.29, associating with the aromatic proton from the newly formed coumarin moiety. Similarly, the characteristic coumarin proton peaks emerged at δ 8.24−8.29 in the spectra of **P2**−**P6** (Figure S7). Furthermore, new characteristic N−H peaks emerged at δ 11.44 (**9**) and 10.71 (**P7**), and NH₂ peaks emerged at δ 6.70 (**9**) and 4.24 (**P7**), proving the amino-substituted quinoline structures in **9** and **P7** (Figure S8). In the ^{13}C NMR spectra of **7**, **8**, and **P1**, the acetylene carbon peaks of **1a** at δ 84.75 and 81.62 disappeared; meanwhile, two new peaks at δ 159.30 and 100.55 appeared, representing the newly formed C═N and C═C bonds on the coumarin moieties of **7**, **8**, and **P1**. The ^{13}C NMR spectra of **P2**−**P7** also suggested the existence of the characteristic C═N and C═C moieties
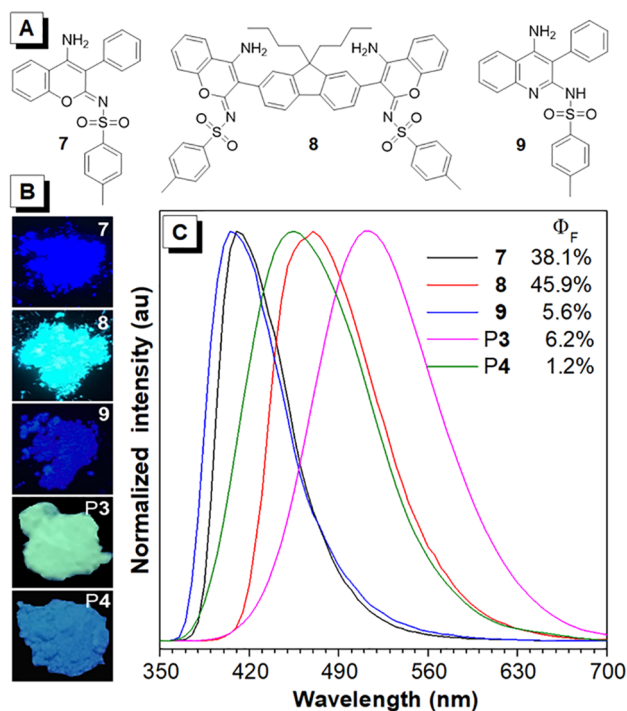
Figure 4. (A) Structures of **7**−**9**. (B) Fluorescence photos of solid powders of **7**−**9**, **P3**, and **P4** taken under UV irradiation at 365 nm. (C) PL spectra and Φ_Fs of solid powders of **7**−**9**, **P3**, and **P4**. Excitation wavelength: 340 nm.
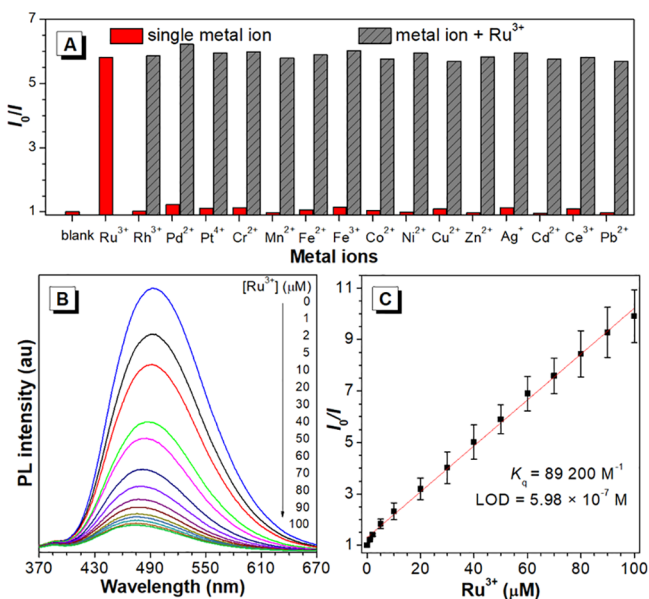

Figure 5. (A) Relative intensity (I_0/I) of aqueous solution of **P3** vs different metal ions. I_0 = PL intensity in the absence of metal ions. Metal ion concentration: 50 μM. (B) PL spectra of **P3** in DMSO/ water mixture with 50 vol % water and different amounts of Ru^{3+}. (C) Stern−Volmer plot of relative intensity (I_0/I) vs the Ru^{3+} concentration. Polymer concentration: 10 μM.

on coumarin or quinoline structure in the polymers (Figures S9 and S10).

Despite of the rigid conjugated fragments and potential hydrogen bonds, these poly(*N*-sulfonylimine)s possess satisfactory solubility in polar organic solvents such as DMSO and DMF. Thermogravimetric analysis also suggests their high
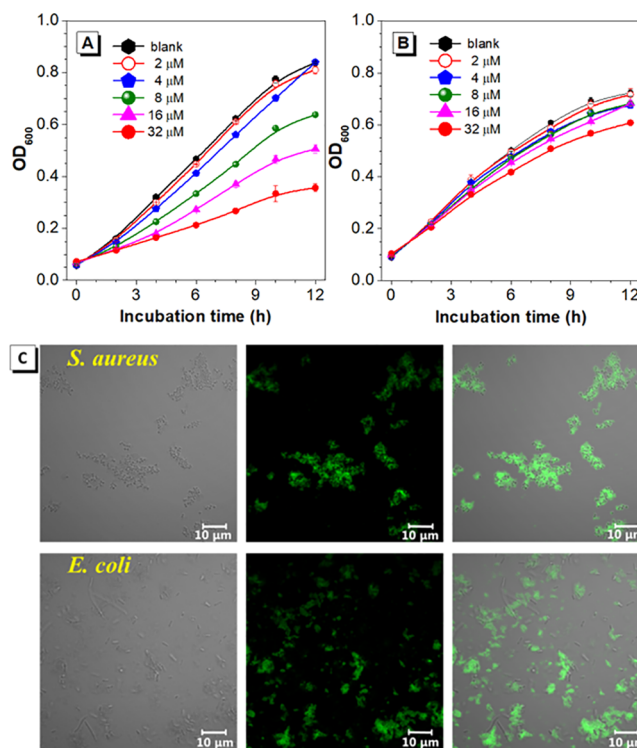

Figure 6. Growth curves of (A) *S. aureus* or (B) *E. coli* incubated with different concentrations of **P3**. (C) CLSM images of *S. aureus* or *E. coli* incubated with **P3**. Left, phase contrast bright-field image; middle, fluorescence images; right, overlap image. Concentration: 10 μM.

thermal stability with decomposition temperatures (T_d) at 5% weight loss ranging from 272 to 344 °C (Figure S11).

The photophysical properties of the model compounds and polymers were then studied. The absorption maxima of the dilute DMSO solutions of **7**−**9** and **P1**−**P7** were measured that were located at 320−350 nm (Figure S12). The solid powders of **7**−**9**, **P3**, and **P4** are emissive, while their DMSO solutions are nonemissive or weakly emissive. No emission is observed from other polymers. The emission maxima of solid powders of **7** and **9** are located at ∼410 nm, while that of **8** and **P4** are red-shifted to 470 and 455 nm, respectively, suggesting elongated conjugation (Figure 4). **P3** with tetraphenylethene moieties showed a green emission at ∼513 nm. Their solid-state fluorescence quantum efficiencies (Φ_Fs) suggested that the iminocoumarin derivatives possess higher Φ_F compared with the aminoquinoline derivatives (Figure 4C). Among them, iminocoumarin derivatives **7** and **8** show bright blue emission with high Φ_F of 38.1% and 45.9%, respectively. In mixed solvents with different amounts of poor solvent *n*-hexane or H_2O, upon addition of poor solvent, the emission of iminocoumarin-containing **7**, **8**, and **P3** are generally increased (Figure S13), suggesting their aggregation-induced emission (AIE) characteristics.[33,34]

AIE polymers are extensively studied as fluorescent chemosensors for metal ion detection, owing to their high sensitivity, selectivity, and reliability.[35−37] The fluorescence response of AIE-active **P3** upon coordination with various metal ions are hence investigated, considering that its multiple heteroatoms and amino groups may serve as metal ligands. Into the DMSO/ H_2O mixed solution of **P3** with 50 vol % H_2O, different metal ions such as Ru^{3+}, Rh^{3+}, Pd^{2+}, Pt^{4+}, Cr^{2+}, Mn^{2+}, Fe^{2+}, Fe^{3+}, Co^{2+}, Ni^{2+}, Cu^{2+}, Zn^{2+}, Ag^+, Cd^{2+}, Ce^{3+}, and Pb^{2+} were added.

The fluorescence of P3 was selectively quenched upon the addition of Ru^{3+}, while no significant change was observed with other metal ions. Moreover, the control experiments with the mixture of different metal ions and Ru^{3+} suggested that the fluorescence quenching was only affected by Ru^{3+}, indicating high selectivity of the fluorescence detection of Ru^{3+} (Figure 5A). Different amounts of $RuCl_3$ were then added into the same solution of P3. When increasing the concentration of $RuCl_3$ from 0 to 100 μM, the emission intensity of P3 decreased, while keeping the spectral profile unchanged (Figure 5B). The Stern−Volmer plot of relative PL intensity (I_0/I) versus the concentration of Ru^{3+} was a straight line. The quenching constant and the calculated detection of limit (LOD) were 89200 M^{-1} and 5.98×10^{-7} M, respectively, suggesting high sensitivity of Ru^{3+} detection (Figure 5C). The emission of P3 and the absorption of $RuCl_3$ in $DMSO/H_2O$ mixture with 50 vol % water content overlaps at the wavelength range of 400−650 nm (Figure S14), indicating potential energy transfer from P3 to Ru^{3+}, which may be the reason for fluorescence quenching.

The iminocoumarin derivatives are well-known compounds with pharmacological properties.[38] The antibacterial property of 4-amino-iminocoumarin-containing fluorescent P3 was hence investigated. Gram-positive bacterium *S. aureus* and Gram-negative bacterium *E. coli* were selected to be incubated with different amounts of P3 (Figure 6A,B). P3 showed an obvious inhibitory effect on the growth of *S. aureus* and the calculated inhibition ratio can reach 58% when *S. aureus* was incubated with 32 μM of P3 for 12 h. The growth of *E. coli*, on the other hand, was not inhibited significantly upon incubation with P3. The confocal laser scanning microscopy (CLSM) images of *S. aureus* or *E. coli* after incubation with P3 suggested that the fluorescent polymer aggregates were located around *S. aureus*, while the fluorescence image of P3 and the bright-field bacteria image were not overlapped for *E. coli* (Figure 6C). The structure of P3 may endow it unique interaction with *S. aureus*, enabling its accumulation around *S. aureus* and further inhibition on the growth of the bacteria.

In this work, efficient one-pot multicomponent polymerizations of diynes, disulfonyl azides, and 2-hydroxybenzonitrile/2-aminobenzonitrile were developed under mild condition at 40 °C in CH_2Cl_2 with the catalysis of CuCl and Et_3N, affording iminocoumarin/aminoquinoline-containing poly(*N*-sulfonylimine)s with high M_ws in excellent yields and releasing N_2 as the only byproduct. The poly(*N*-sulfonylimine)s enjoyed good solubility and good thermal stability. The iminocoumarin and aminoquinoline structures that built directly from the MCP could be interesting fluorophores, evidenced by the aggregation-induced emission property of the corresponding model compounds. Moreover, the fluorescent poly(*N*-sulfonylimine)s can be utilized in fluorescence detection of Ru^{3+}, and the inhibition of the growth of bacteria such as *S. aureus*. It is anticipated that these MCPs may find potential application in material science by bringing polymers with unique structures and advanced functionalities.

■ ASSOCIATED CONTENT

Ⓢ Supporting Information

The Supporting Information is available free of charge on the ACS Publications website at DOI: 10.1021/acsmacro-lett.8b00884.

Materials and instrumentation; experimental procedures and characterization data; polymerization condition optimization on solvent, concentration, time, monomer feeding ratio, and temperature; GPC curves of P1−P7; Synthesis and MS spectra of 7−9; IR, ^1H NMR, and ^{13}C NMR spectra of P2−P7; TGA thermograms and absorption spectra of P1−P7; PL spectra of 7, 8, and P3 in mixed solvents with different content of poor solvent; absorption spectra of $RuCl_3$ (PDF).

■ AUTHOR INFORMATION

Corresponding Authors
*E-mail: msrrhu@scut.edu.cn.
*E-mail: tangbenz@ust.hk.

ORCID Ⓞ
Rongrong Hu: 0000-0002-7939-6962
Ben Zhong Tang: 0000-0002-0293-964X

Notes
The authors declare no competing financial interest.

■ REFERENCES

(1) Hu, R.; Li, W.; Tang, B. Z. Recent Advances in Alkyne-Based Multicomponent Polymerizations. *Macromol. Chem. Phys.* **2016**, *217*, 213−224.

(2) Llevot, A.; Boukis, A. C.; Oelmann, S.; Wetzel, K.; Meier, M. A. An Update on Isocyanide-Based Multicomponent Reactions in Polymer Science. *Top. Curr. Chem.* **2017**, *375*, 66−94.

(3) Rotstein, B. H.; Zaretsky, S.; Rai, V.; Yudin, A. K. Small Heterocycles in Multicomponent Reactions. *Chem. Rev.* **2014**, *114*, 8323−8359.

(4) Estevez, V.; Villacampa, M.; Menendez, J. C. Recent Advances in the Synthesis of Pyrroles by Multicomponent Reactions. *Chem. Soc. Rev.* **2014**, *43*, 4633−4657.

(5) Xue, H.; Zhao, Y.; Wu, H.; Wang, Z.; Yang, B.; Wei, Y.; Wang, Z.; Tao, L. Multicomponent Combinatorial Polymerization via the Biginelli Reaction. *J. Am. Chem. Soc.* **2016**, *138*, 8690−8693.

(6) Kreye, O.; Toth, T.; Meier, M. A. Introducing Multicomponent Reactions to Polymer Science: Passerini Reactions of Renewable Monomers. *J. Am. Chem. Soc.* **2011**, *133*, 1790−1792.

(7) Deng, X. X.; Li, L.; Li, Z. L.; Lv, A.; Du, F. S.; Li, Z. C. Sequence Regulated Poly(ester-amide)s Based on Passerini Reaction. *ACS Macro Lett.* **2012**, *1*, 1300−1303.

(8) Sehlinger, A.; Dannecker, P.-K.; Kreye, O.; Meier, M. A. Diversely Substituted Polyamides: Macromolecular Design Using the Ugi Four-Component Reaction. *Macromolecules* **2014**, *47*, 2774−2783.

(9) Wei, B.; Li, W.; Zhao, Z.; Qin, A.; Hu, R.; Tang, B. Z. Metal-Free Multicomponent Tandem Polymerizations of Alkynes, Amines, and Formaldehyde toward Structure- and Sequence-Controlled Luminescent Polyheterocycles. *J. Am. Chem. Soc.* **2017**, *139*, 5075−5084.

(10) Tang, X.; Zheng, C.; Chen, Y.; Zhao, Z.; Qin, A.; Hu, R.; Tang, B. Z. Multicomponent Tandem Polymerizations of Aromatic Diynes, Terephthaloyl Chloride, and Hydrazines toward Functional Conjugated Polypyrazoles. *Macromolecules* **2016**, *49*, 9291−9300.

(11) Zheng, C.; Deng, H.; Zhao, Z.; Qin, A.; Hu, R.; Tang, B. Z. Multicomponent Tandem Reactions and Polymerizations of Alkynes,

Carbonyl Chlorides, and Thiols. *Macromolecules* **2015**, *48*, 1941−1951.

(12) Tian, T.; Hu, R.; Tang, B. Z. Room Temperature One-Step Conversion from Elemental Sulfur to Functional Polythioureas through Catalyst-Free Multicomponent Polymerizations. *J. Am. Chem. Soc.* **2018**, *140*, 6156−6163.

(13) Li, W.; Wu, X.; Zhao, Z.; Qin, A.; Hu, R.; Tang, B. Z. Catalyst-Free, Atom-Economic, Multicomponent Polymerizations of Aromatic Diynes, Elemental Sulfur, and Aliphatic Diamines toward Luminescent Polythioamides. *Macromolecules* **2015**, *48*, 7747−7754.

(14) Xu, L.; Hu, R.; Tang, B. Z. Room Temperature Multicomponent Polymerizations of Alkynes, Sulfonyl Azides, and Iminophosphorane toward Heteroatom-Rich Multifunctional Poly-(phosphorus amidine)s. *Macromolecules* **2017**, *50*, 6043−6053.

(15) Xu, L.; Zhou, F.; Liao, M.; Hu, R.; Tang, B. Z. Room Temperature Multicomponent Polymerizations of Alkynes, Sulfonyl Azides, and N-Protected Isatins toward Oxindole-Containing Poly(N-acylsulfonamide)s. *Polym. Chem.* **2018**, *9*, 1674−1683.

(16) Han, T.; Deng, H.; Qiu, Z.; Zhao, Z.; Zhang, H.; Zou, H.; Leung, N. L. C.; Shan, G.; Elsegood, M. R. J.; Lam, J. W. Y.; Tang, B. Z. Facile Multicomponent Polymerizations toward Unconventional Luminescent Polymers with Readily Openable Small Heterocycles. *J. Am. Chem. Soc.* **2018**, *140*, 5588−5598.

(17) Lee, I. H.; Kim, H.; Choi, T. L. Cu-Catalyzed Multicomponent Polymerization to Synthesize a Library of Poly(N-sulfonylamidines). *J. Am. Chem. Soc.* **2013**, *135*, 3760−3763.

(18) Kim, H.; Choi, T. L. Preparation of a Library of Poly(N-sulfonylimidates) by Cu-Catalyzed Multicomponent Polymerization. *ACS Macro Lett.* **2014**, *3*, 791−794.

(19) Komatsu, K.; Urano, Y.; Kojima, H.; Nagano, T. Development of an Iminocoumarin-Based Zinc Sensor Suitable for Ratiometric Fluorescence Imaging of Neuronal Zinc. *J. Am. Chem. Soc.* **2007**, *129*, 13447−13454.

(20) Singh, I.; Kaur, H.; Kumar, S.; Kumar, A.; Lata, S.; Kumar, A. Synthesis of New Coumarin Derivatives as Antibacterial Agents. *Int. J. Chem. Technol. Res.* **2010**, *2*, 1745−1752.

(21) De Souza, M. V.; Pais, K. C.; Kaiser, C. R.; Peralta, M. A.; Ferreira, M. D. L.; Lourenço, M. C. Synthesis and in Vitro Antitubercular Activity of a Series of Quinoline Derivatives. *Bioorg. Med. Chem.* **2009**, *17*, 1474−1480.

(22) Kirkiacharian, S.; Thuy, D. T.; Sicsic, S.; Bakhchinian, R.; Kurkjian, R.; Tonnaire, T. Structure−Activity Relationships of Some 3-substituted-4-hydroxycoumarins as HIV-1 Protease Inhibitors. *Farmaco* **2002**, *57*, 703−708.

(23) Heiniger, B.; Gakhar, G.; Prasain, K.; Hua, D. H.; Nguyen, T. A. Second-Generation Substituted Quinolines as Anticancer Drugs for Breast Cancer. *Anticancer Res.* **2010**, *30*, 3927−3932.

(24) Burke, T. R.; Lim, B.; Marquez, V. E.; Li, Z. H.; Bolen, J. B.; Stefanova, I.; Horak, I. D. Bicyclic Compounds as Ring-Constrained Inhibitors of Protein-Tyrosine Kinase p56[lck]. *J. Med. Chem.* **1993**, *36*, 425−432.

(25) Kim, J. L.; Cho, H. N.; Kim, J. K.; Hong, S. I. New Quinoline-Based Alternating Copolymers Containing a Fluorene Unit. *Macromolecules* **1999**, *32*, 2065−2067.

(26) Jégou, G.; Jenekhe, S. A. Highly Fluorescent Poly(arylene ethynylene)s Containing Quinoline and 3-Alkylthiophene. *Macromolecules* **2001**, *34*, 7926−7928.

(27) Deng, H.; Han, T.; Zhao, E.; Kwok, R. T. K.; Lam, J. W. Y.; Tang, B. Z. Multicomponent Click Polymerization: A Facile Strategy toward Fused Heterocyclic Polymers. *Macromolecules* **2016**, *49*, 5475−5483.

(28) Yi, F.; Zhang, S.; Huang, Y.; Zhang, L.; Yi, W. An Efficient One-Pot Protocol for the Synthesis of Polysubstituted 4-Amino-iminocoumarins and 4-Aminoquinolines by a Copper-Catalyzed Three-Component Reaction. *Eur. J. Org. Chem.* **2017**, *1*, 102−110.

(29) Bae, I.; Han, H.; Chang, S. Highly Efficient One-Pot Synthesis of N-Sulfonylamidines by Cu-Catalyzed Three-Component Coupling of Sulfonyl Azide, Alkyne, and Amine. *J. Am. Chem. Soc.* **2005**, *127*, 2038−2039.

(30) Yao, B.; Mei, J.; Li, J.; Wang, J.; Wu, H.; Sun, J. Z.; Qin, A.; Tang, B. Z. Catalyst-Free Thiol−Yne Click Polymerization: A Powerful and Facile Tool for Preparation of Functional Poly(vinylene sulfide)s. *Macromolecules* **2014**, *47*, 1325−1333.

(31) Wang, J.; Li, B.; Xin, D.; Hu, R.; Zhao, Z.; Qin, A.; Tang, B. Z. Superbase Catalyzed Regio-Selective Polyhydroalkoxylation of Alkynes: A Facile Route towards Functional Poly(vinyl ether)s. *Polym. Chem.* **2017**, *8*, 2713−2722.

(32) Katritzky, A. R.; Rogers, J. W.; Witek, R. M.; Vakulenko, A. V.; Mohapatra, P. P.; Steel, P. J.; Damavarapu, R. Synthesis and Characterization of Blowing Agents and Hypergolics. *J. Energ. Mater.* **2007**, *25*, 79−109.

(33) Luo, J.; Xie, Z.; Lam, J. W. Y.; Cheng, L.; Tang, B. Z.; Chen, H.; Qiu, C.; Kwok, H. S.; Zhan, X.; Liu, Y.; Zhu, D. Aggregation-Induced Emission of 1-Methyl-1,2,3,4,5-pentaphenylsilole. *Chem. Commun.* **2001**, 1740−1741.

(34) Mei, J.; Leung, N. L.; Kwok, R. T.; Lam, J. W.; Tang, B. Z. Aggregation-Induced Emission: Together We Shine, United We Soar! *Chem. Rev.* **2015**, *115*, 11718−11940.

(35) Liu, Y.; Roose, J.; Lam, J. W.; Tang, B. Z. Multicomponent Polycoupling of Internal Diynes, Aryl Diiodides, and Boronic Acids to Functional Poly(tetraarylethene)s. *Macromolecules* **2015**, *48*, 8098−8107.

(36) Saha, S. K.; Ghosh, K. R.; Gao, J. P.; Wang, Z. Y. Highly Sensitive Dual-Mode Fluorescence Detection of Lead Ion in Water Using Aggregation-Induced Emissive Polymers. *Macromol. Rapid Commun.* **2014**, *35*, 1592−1597.

(37) Liu, Y. L.; Wang, Z. K.; Qin, W.; Hu, Q. L.; Tang, B. Z. Fluorescent Detection of Cu (II) by Chitosan-Based AIE Bioconjugate. *Chin. J. Polym. Sci.* **2017**, *35*, 365−371.

(38) Srikrishna, D.; Godugu, C.; Dubey, P. K. A Review on Pharmacological Properties of Coumarins. *Mini-Rev. Med. Chem.* **2018**, *18*, 113−141.